Progress of Theoretical Physics, Vol. 121, No. 4, April 2009

Topological Entropy in a Parameter Range of the Standard Map

Yoshihiro YAMAGUCHI[1] and Kiyotaka TANIKAWA[2]

[1] *Teikyo Heisei University, Tokyo 170-8445, Japan*
[2] *National Astronomical Observatory, Mitaka 181-8588, Japan*

(Received December 11, 2008)

We combine the trellis method and the braid method, and by estimating the lower bounds of the topological entropy of the standard map for a certain parameter range, we follow the change of the topological entropy. The trellis in a tangency situation of the stable and unstable manifolds is constructed. Applying the trellis method to this trellis, the lower bound of topological entropy is calculated. There exist systems in which the trellis method can not be applicable. For such systems, we look for non-Birkhoff periodic orbits existent in the trellises, form braids from those periodic orbits, and estimate the topological entropy from their braid types. We perform these tasks for a sequence of trellises and numerically visualize the change in the topological entropy. In addition, we take particular sequence of connecting orbits to obtain homoclinic or heteroclinic orbits. As a natural extension, we assign topological entropy to these homoclinic and heteroclinic orbits.

Subject Index: 030

§1. Introduction

It is natural to measure the degree of chaos using the topological entropy. In the two-dimensional maps, we can use two methods, called the trellis method[1)] and the braid method,[2)] to estimate a lower bound for the topological entropy of the systems given by the maps. These two methods have different utilities. In some situations, the trellis method is advantageous, while in other situations, the braid method is appropriate.

Using the arcs of the stable and unstable manifolds, we construct a trellis and apply the method proposed by Collins to the trellis when there is a tangency situation of stable and unstable manifolds of a fixed point. We form a transition matrix among areas in the trellis and then obtain the topological entropy. This method is useful for estimating the topological entropy during the formation of the twofold horseshoe in the Hénon map[3)] or of the threefold horseshoe in the cubic map[4)] or the standard map. A trellis is a compact object. Hence, the trellis method is applicable to the orbits in the compact region of the phase space.

On the other hand, we can use the braid method for a non-Birkhoff periodic orbit whose rotation number is positive or negative, which means that the orbit is not confined in the compact region in the universal cover. Using the permutation order of the non-Birkhoff periodic orbit, we construct the braid and obtain the braid type. Applying the Burau matrix method[2),5)] or the train-track method[6)] to the braid type, we can estimate the topological entropy. One difficulty in this method is that it is not so easy to find non-Birkhoff periodic orbits in a given system.

In order to represent our purpose in detail, we use the standard map. We, from the beginning, lift the map to the universal cover $\boldsymbol{R} \times \boldsymbol{R}$ with coordinates (x, y). Then, the standard map T is defined by

$$y_{n+1} = y_n + f(x_n), \tag{1·1}$$

$$x_{n+1} = x_n + y_{n+1}, \tag{1·2}$$

where $f(x) = a \sin x$ and a is a positive parameter. There are two fixed points, $P = (0, 0)$ and $Q = (\pi, 0)$, in the cylinder, where P is a saddle and Q is an elliptic point or a saddle with reflection. In the universal cover, P and Q have copies $P_{k,j}$ at $(2\pi k, 2\pi j)$ and $Q_{k,j}$ at $(2\pi k + \pi, 2\pi j)$ for any k, j. There exist stable and unstable manifolds for $P_{0,0}$ and its copies. We denote by W_u the branch of the unstable manifold of $P_{0,0}$ going to the upper-right direction, and by W_s the branch of the stable manifold of the saddle $P_{1,0}$ coming from the upper-left direction. In Fig. 1, the unstable manifold is illustrated with a thick curve and the stable manifold by a thin curve.

We consider two particular tangency situations displayed in Fig. 1. The first situation is displayed in Fig. 1(a), where the unstable manifold W_u of $P_{0,0}$ and the symmetry axis $x = 2\pi$ have a tangency point named s. The trellis is formed by the two arcs $[P_{0,0}, s]$ of the unstable manifold of $P_{0,0}$ and arc $[P_{2,0}, s]$ of the stable manifold of the saddle $P_{2,0}$. The tangency point s is a homoclinic point. In Fig. 1(b), the heteroclinic tangency situation is displayed, where t is a heteroclinic point. The trellis is formed by the two arcs $[P_{0,0}, t]$ of the unstable manifold of $P_{0,0}$ and arc $[P_{1,1}, t]$ of the stable manifold of the saddle $P_{1,1}$. For both situations, we cannot use the trellis method since the tangency point s and t rotate the cylinder, and thus their orbits are not bounded in the universal cover. We propose a method of calculating the topological entropy for these situations. Our method is summarized below.

Our Method

First step: We set up a situation of homoclinic/heteroclinic tangency, and take a trellis $\mathcal{T}$ constructed by arcs of the stable and unstable manifolds.

Second step: Using information on the behavior of areas of $\mathcal{T}$ under the map, we find a non-Birkhoff periodic orbit with rotation number p/q (abbreviated as p/q-NB).

Third step: Using the orbital order of p/q-NB, we construct the braid and obtain its braid type.

Fourth step: We calculate the topological entropy in terms of the Burau matrix method or the train-track method. The program code of the Burau matrix method is obtained from Ref. 5). We also use the software, *Trains3*, proposed by Hall.[7)]

By our method, we obtain the following results:

[1] The lower bound for topological entropy is $\ln 2$ for the situation displayed in Fig. 1(a).

[2] The lower bound for topological entropy is $\ln(\sqrt{2} + 1)$ in the situation displayed in Fig. 1(b).

In §2, we summarize the mathematical tools used in §§3 and 4. We prove the existence of the non-Birkhoff periodic orbits forced by $\mathcal{T}$ in §3. The braid type of the non-Birkhoff periodic orbit is determined and the topological entropy is calculated

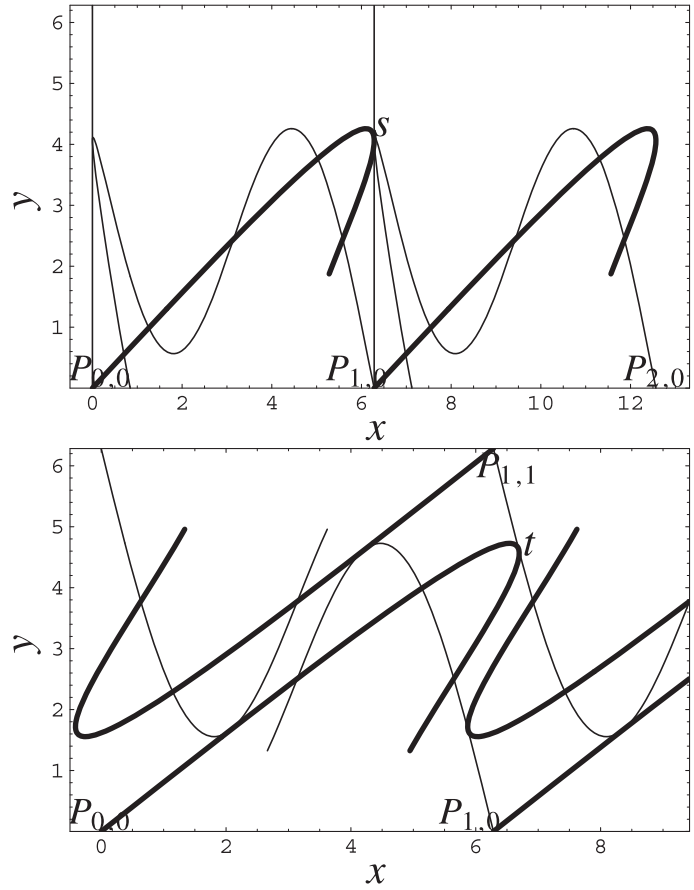

Fig. 1. In the universal cover, the unstable manifold (thick curves) and the stable manifold (thin curves) are displayed. (a) Arc $[P_{0,0}, s]$ of the unstable manifold of $P_{0,0}$ and arc $[P_{2,0}, s]$ of the stable manifold of the saddle $P_{2,0}$ form a trellis ($a = 2.920$). (b) Arc $[P_{0,0}, t]$ of the unstable manifold of $P_{0,0}$ and arc $[P_{1,1}, t]$ of the stable manifold of the saddle $P_{1,1}$ form a trellis ($a = 3.368$).

in §4. Applying our method to various trellises, we calculate the topological entropy in §5. Using the findings presented derived in §3, the order relation between the connecting orbits is obtained in §6.

§2. Several mathematical tools

The material in this section is almost the same as that in Ref. 8). We include this for the convenience of the reader.

2.1. *Symmetry axes and symmetric periodic orbits*

The standard map is represented as a product of two involutions H and G:[9]

$$T = H \circ G, \tag{2·1}$$

$$G(x,y) = (-x, y + f(x)), \tag{2·2}$$
$$H(x,y) = (y - x, y). \tag{2·3}$$

The symmetry axes are the set of fixed points of H and G, and in the universal cover, these are given by

$$S_G(k) : x = k\pi, \tag{2·4}$$
$$S_H(k) : y = 2(x - k\pi) \tag{2·5}$$

for $k \in \boldsymbol{Z}$. In the following, we set $S_{G,H}(k)$ as the part of the symmetry axes located in the region satisfying $y > 0$.

We consider two expressions for orbits in the universal cover. One is the (simple) orbit $O(z)$ of a point z:

$$O(z) = \{\ldots, T^{-1}z, z, Tz, \ldots\}. \tag{2·6}$$

The other is the extended orbit $EO(z)$ of a point z:[10)]

$$EO(z) = \{T^k z + (2\pi l, 0) : k, l \in \boldsymbol{Z}\}. \tag{2·7}$$

The point z is called a p/q-periodic point if

$$T^q z - (2\pi p, 0) = z. \tag{2·8}$$

The quantity p/q $(0 < p/q < 1)$ is the rotation number of the orbit.

Let us consider a p/q-periodic point z. If two points of $T^i z$ $(i = 0, \ldots, q-1)$ are on the symmetry axes, we call its orbit a *symmetric p/q-periodic orbit*. We are concerned with symmetric periodic orbits starting at $S_G(k)$ or $S_H(k)$ $(k \in \boldsymbol{Z})$. Let us give the basic properties of a symmetric p/q-periodic orbit.[9)]

Property 2.1.1
(i) Suppose that z is located on $S_G(k_1)$ and $T^n z$ $(n \geq 1)$ is located on $S_H(k_2)$, but that no $T^i z$ for $0 < i < n$ is located on a symmetry axis. Then the period is $q = 2n - 1$, and the rotation number is $p/q = (k_2 - k_1)/(2n - 1)$. Suppose that z is located on $S_H(k_1)$ and $T^n z$ $(n \geq 1)$ is located on $S_G(k_2)$, but that no $T^i z$ for $0 < i < n$ is located on a symmetry axis. Then the period is $q = 2n + 1$, and the rotation number is $p/q = (k_2 - k_1)/(2n + 1)$.
(ii) Suppose that z is located on $S_G(k_1)$ and $T^n z$ $(n \geq 1)$ is located on $S_G(k_2)$, but that no $T^i z$ for $0 < i < n$ is located on a symmetry axis. Then the period is $q = 2n$, and the rotation number is $p/q = (k_2 - k_1)/(2n)$. Suppose that z is located on $S_H(k_1)$ and $T^n z$ $(n \geq 1)$ is located on $S_H(k_2)$ $(n \geq 2)$, but that no $T^i z$ for $0 < i < n$ is located on a symmetry axis. Then the period is $q = 2n$, and the rotation number is $p/q = (k_2 - k_1)/(2n)$.

2.2. *Birkhoff and non-Birkhoff periodic orbits*

An extended orbit $EO(z)$ is said to be *monotone* if for any two points, $r, s \in EO(z)$,

$$\pi_x(r) < \pi_x(s) \text{ implies } \pi_x(Tr) < \pi_x(Ts), \tag{2·9}$$

where $\pi_x(r)$ is the x-coordinate of r. If there exists a pair of points r and s not satisfying Eq. (2·9), we call the orbit a *nonmonotone orbit*. If the orbit is periodic and monotone, we call it a *monotone periodic orbit* or a *Birkhoff periodic orbit*. If it is nonmonotone, we call it a *nonmonotone periodic orbit* or a *non-Birkhoff periodic orbit*. If, in addition, an irreducible rotation number p/q is given, the Birkhoff periodic orbit is called a p/q-Birkhoff periodic orbit, and it is denoted by p/q-B.

We denote the elliptic periodic orbit as p/q-BE and the saddle orbit as p/q-BS. It is well known that there are (at least) two p/q-Bs for every irreducible p/q in the monotone twist maps, including the standard map. This is the Poincaré-Birkhoff theorem.[11] In the standard map, there are one symmetric p/q-BE and one symmetric p/q-BS for every irreducible p/q.[12] There are no nonsymmetric p/q-Bs in the standard map. For the brevity of notation, *we write p/q-BEs and p/q-BSs instead of writing symmetric p/q-BEs and p/q-BSs.*

Similarly, a non-Birkhoff periodic orbit with rotation number p/q is called a p/q-non-Birkhoff periodic orbit. *We consider only symmetric p/q-non-Birkhoff periodic orbits in the present paper. Thus, hereafter, these are denoted by p/q-NBs without 'symmetric'.*

2.3. *Resonance regions and non-Birkhoff periodic orbits*

The stable and unstable manifolds of a p/q-BS intersect each other or construct a saddle connection. In the latter case, the separatrix is formed. We note that the stable and unstable manifolds of any p/q-BS intersect transversely with each other for $a > 0$.[13),14)] We construct the resonance region $Z_{p/q}(z_0)$ by using the arcs of the stable and unstable manifolds of the adjacent saddle points (of p/q-BS) of z_0, where z_0 is an orbital point of p/q-BE (see Fig. 2). We call $Z_{p/q}(z_0)$ as the resonance region of z_0. Next, collecting all resonance regions of the orbital points of p/q-BE, the resonance chain $\langle Z_{p/q} \rangle$ is defined. The detailed procedure for constructing the resonance regions is explained in Ref. 8).

2.4. *Symmetric non-Birkhoff periodic orbits*

Suppose that a symmetric p/q-non-Birkhoff periodic orbit has its orbital points only in two resonance chains, $\langle Z_{p_1/q_1} \rangle$ and $\langle Z_{p_2/q_2} \rangle$ with $0 \leq p_1/q_1 < p_2/q_2 \leq 1$ and $p = p_1 + p_2$, $q = q_1 + q_2$. Because of the condition $q = q_1 + q_2$, this orbit has only one orbital point in every resonance region of $\langle Z_{p_1/q_1} \rangle$ and $\langle Z_{p_2/q_2} \rangle$. In this report, we denote this kind of p/q-NB by $p_1/q_1 \oplus p_2/q_2$-NB. That this orbit is actually non-Birkhoff (i.e., nonmonotone) has been proved in Ref. 8). In colloquial words, this orbit rotates the cylinder slowly when its points are in the chain $\langle Z_{p_1/q_1} \rangle$, whereas the orbit moves fast when its points are in the chain $\langle Z_{p_2/q_2} \rangle$.

Next, let $l_{p/q}(k)$ be the arc of the symmetry axis included in the resonance region $Z_{p/q}(z_k)$, where z_k is an orbital point of p/q-BE, and either $z_k \in S_G(k)$ or $z_k \in S_H(k)$ depending on the parity of q. For example, $l_{1/2}(0)$ and $l_{1/3}(0)$ are displayed in Fig. 2, where $l_{1/2}(0) = S_G(0) \cap Z_{1/2}(z_0')$ and $l_{1/3}(0) = S_H(0) \cap Z_{1/3}(z_0)$. Note that the argument 0 of $l_{1/2}(0)$ means $n = 0$ of $S_G(n)$.

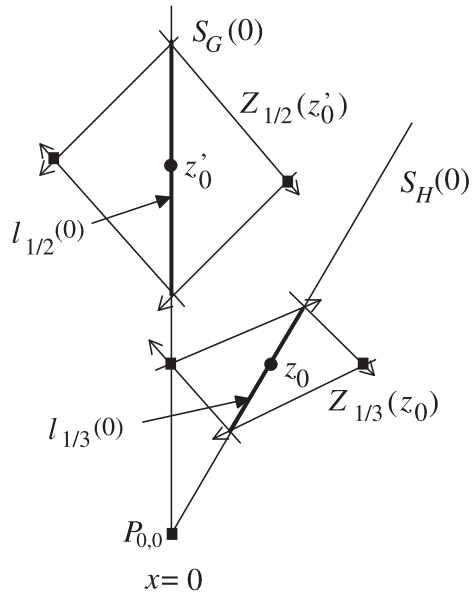

Fig. 2. Arc of symmetry axis included in the resonance region. The two arcs $l_{1/2}(0)$ in $Z_{1/2}(z_0')$ and $l_{1/3}(0)$ in $Z_{1/3}(z_0)$ are displayed where z_0' is an orbital point of 1/2-BE and z_0 is that of 1/3-BE.

§3. Non-Birkhoff periodic orbits forced by trellises

A trellis is a dynamical object formed with stable and unstable arcs of a saddle or saddles. Given a trellis, there exist certain non-Birkhoff periodic orbits. In this sense, we can say that (the existence of) the trellis forces (the existence of) certain non-Birkhoff periodic orbits. In this section, some of these forcing relations are established.

Proposition 3.1.
(i) The trellis displayed in Fig. 1(a) forces any $p/q \oplus 1/2$-NB with $0 < p/q < 1/2$.
(ii) The trellis displayed in Fig. 1(b) forces any $p/q \oplus r/s$-NB with $0 < p/q < r/s < 1$.
Outline of Proof. The detailed proof is long. Its essential parts are in Ref. 8). Here, we give the outline of the proof of Proposition 3.1(i).

Let us first consider the case where q is even, and let $q = 2m$ $(m \geq 2)$. We take the initial point z_0 of p/q-BE on $S_G(-p+1)$. Then we have $l_{p/q}(-p+1) = Z_{p/q}(z_0) \cap S_G(-p+1)$. From the definition of the resonance region, $T^k l_{p/q}(-p+1)$ belongs to $Z_{p/q}(z_k)$ for $k = 1, 2, \ldots, m$, while arc $T^{m+1} l_{1/2}(-p+1)$ is no longer confined in the resonance region. Its form is restricted by Γ_u, which is the arc of W_u with two terminals u and v on W_s, as illustrated in Fig. 3. More precisely, $T^{m+1} l_{1/2}(-p+1) \cap V = \emptyset$, where V is the homoclinic lobe formed by Γ_u and arc $[u, v]_{W_s}$. We set up the situation so that Γ_u is tangent to $S_G(2)$ (see Figs. 1(a) and 3). This implies that $T^{m+1} l_{1/2}(-p+1)$ intersects $S_G(2)$ at two points. From Property 2.1.1(ii), the intersection points (open squares on $S_G(2)$ in Fig. 3) are the

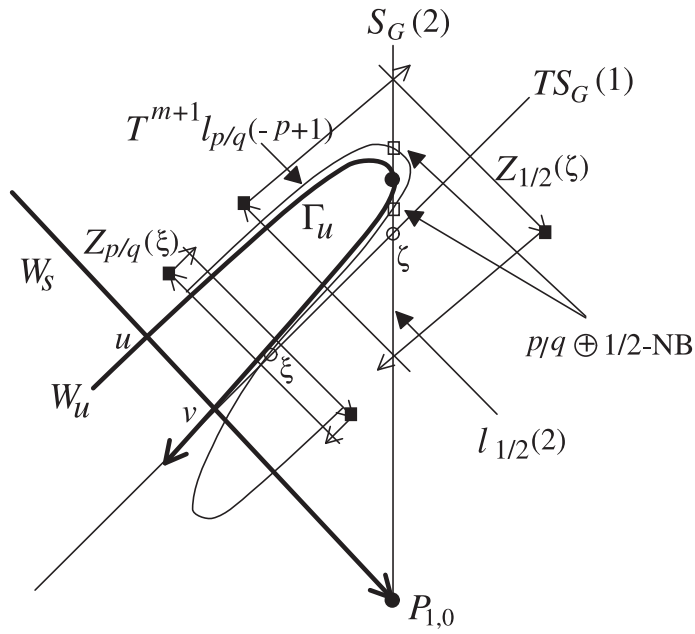

Fig. 3. Resonance regions $Z_{1/2}(\zeta)$ and $Z_{p/q}(\xi)$ around $TS_G(1)$ in the situation of Fig. 1(a), where ζ is the orbital point of 1/2-BE and ξ is that of p/q-BE. The intersection points displayed by open squares in $Z_{1/2}(\zeta)$ are the orbital points of $p/q \oplus 1/2$-NBs.

orbital points of $p/q \oplus 1/2$-NBs with period $2m+2$.

If q is odd, i.e., $q = 2m+1$ $(m \geq 1)$, we take initial point z_0 of p/q-BE on $S_H(-p+1)$, and define $l_{1/2}(-p+1) = Z_{p/q}(z_0) \cap S_H(-p+1)$. The following argument is completely parallel to the case of even q. We obtain two intersection points of $T^m l_{1/2}(-p+1)$ and $S_G(2)$. From Property 2.1.1(i), the intersection points are the orbital points of $p/q \oplus 1/2$-NBs with period $(2m+1)+2$. (Q.E.D.)

§4. Braid types and topological entropy

In order to calculate the topological entropy of the standard map for a given parameter value, we construct a braid from a non-Birkhoff periodic orbit that exists for this parameter value. The corresponding braid is uniquely determined if the order of orbital points projected to the cylinder, or the permutation order, is known. However, in the general case, it is very difficult to know the exact order. Fortunately, we have the results obtained by Boyland.[15),16)] Boyland, similarly to us, constructed a new periodic orbit of rotation number p/q by joining two monotone periodic orbits with rotation numbers p_1/q_1 and p_2/q_2 $(0 < p_1/q_1 < p_2/q_2 < 1)$ such that $p = p_1 + p_2$ and $q = q_1 + q_2$. He proved that the joined periodic orbit has the minimum topological entropy if q_1 points move with rigid rotation and then q_2 points move with rigid rotation. Nonmonotonicity of the orbit comes from the transition between two rigid rotations. This gives rise to the nonzero topological entropy. Boyland proved this

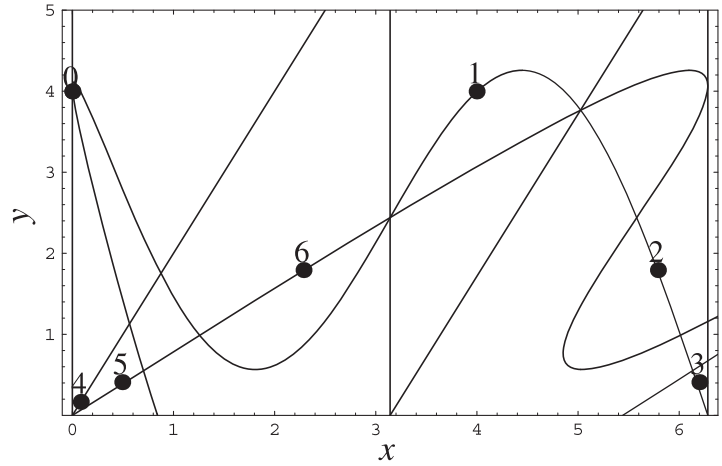

Fig. 4. Orbital points of $1/5 \oplus 1/2$-NB forced by $\mathcal{T}$ displayed in Fig. 1(a). Here, i stands for $\tilde{z}_i$ in the cylinder. The two points $\tilde{z}_0$ and $\tilde{z}_1$ are located in $\langle Z_{1/2} \rangle$ and the five points $\tilde{z}_i$ $(2 \leq i \leq 6)$ are in $\langle Z_{1/5} \rangle$.

for the case of $p = 2$, $q = 5$, $p_1 = p_2 = 1$, $q_1 = 3$, and $q_2 = 2$ in Ref. 15) and for the general case in Ref. 16).

Our setting of the problem is the same as Boyland's. However, we are treating the actual map, i.e., the standard map. Although p_1/q_1-BE and p_2/q_2-BE are monotone, the rotation of their orbital points is not rigid. Hence, the projected points of the joined periodic orbit may not necessarily be ordered as those of rigid rotation. The order of points may have deviations from the expected order. Our task here is to show that deviated orders do not affect the value of the topological entropy.

Let us first explain how to determine the permutation order for a given non-Birkhoff periodic orbit, using $1/5 \oplus 1/2$-NB as an example. Let $\tilde{z}_i = (\tilde{x}_i, y_i)$ $(0 \leq i \leq 6)$ be the orbital points of $1/5 \oplus 1/2$-NB, where $\tilde{z}_i$ denotes the projection to the cylinder and $\tilde{x}_i$ means the value modulo 2π. Orbital points $\tilde{z}_0$ and $\tilde{z}_1$ are located in $\langle Z_{1/2} \rangle$ and points $\tilde{z}_i$ for $2 \leq i \leq 6$ are in $\langle Z_{1/5} \rangle$ (see Fig. 4). We take the permutation order of 1/5-BE as a candidate of the simplest permutation order when the points are in the resonance region of $\langle Z_{1/5} \rangle$, whereas the permutation order is that of 1/2-BE when the points are in the resonance region of $\langle Z_{1/2} \rangle$.

If two rigid motions are concatenated, points $\tilde{z}_1$ and $\tilde{z}_6$ are located in $S_G(1)$. In reality, these points are outside $S_G(1)$. Let us examine this in what follows. From the fact that $\tilde{z}_1$ is located in $\langle Z_{1/2} \rangle$ and $\tilde{z}_2$ in $\langle Z_{1/5} \rangle$, the orbital points should jump from $\langle Z_{1/2} \rangle$ down to $\langle Z_{1/5} \rangle$. This implies relations $y_2 < y_1$ and $\tilde{x}_1 > \pi$, i.e., $\tilde{z}_1$ is located to the right of $S_G(1)$. On the other hand, $\tilde{z}_6$ is located in $\langle Z_{1/5} \rangle$, and $\tilde{z}_7$ $(= \tilde{z}_0)$ in $\langle Z_{1/2} \rangle$. Thus, the orbital points should jump from $\langle Z_{1/5} \rangle$ up to $\langle Z_{1/2} \rangle$. Therefore, $\tilde{z}_6$ is located to the left of $S_G(1)$. Then, we obtain relations $\tilde{x}_6 < \pi < \tilde{x}_1$, as shown in Fig. 4. It is noted that the relation $\tilde{z}_k = G\tilde{z}_{7-k}$ holds, where the symmetry axis of G is $S_G(1)$. Thus, we have the following relations,

$$0 = \tilde{x}_0 < \tilde{x}_4 < \tilde{x}_5 < \tilde{x}_6 < \pi < \tilde{x}_1 < \tilde{x}_2 < \tilde{x}_3 < 2\pi. \tag{4·1}$$

We represent these order relations for $\tilde{x}_i$ $(0 \leq i \leq 6)$ as $\mathrm{Perm}(1/5 \oplus 1/2) = \{0, 4, 5, 6, 1, 2, 3\}$, and call this the permutation order of $1/5 \oplus 1/2$-NB. This permutation order is the $(1/5, 1/2)$ concatenation order structure defined by Boyland[15] and corresponds to the minimal topological entropy among other permutation orders. Let us denote the corresponding motion of points by the *rigid motion approximation*.

We can construct the braid of $1/5 \oplus 1/2$-NB with $\mathrm{Perm}(1/5 \oplus 1/2)$ (see Fig. 5).

In Fig. 5, the part of a strand illustrated by the dashed line represents the fact that the orbit moves around the rear side of the cylinder. The strand from $\tilde{z}_0$ to $\tilde{z}_1$ overtakes two strands from $\tilde{z}_4$ to $\tilde{z}_5$ and from $\tilde{z}_5$ to $\tilde{z}_6$. In such situations, the strand from $\tilde{z}_0$ to $\tilde{z}_1$ goes behind two strands from $\tilde{z}_4$ to $\tilde{z}_5$ and from $\tilde{z}_5$ to $\tilde{z}_6$. The strand from $\tilde{z}_6$ to $\tilde{z}_0$ $(\tilde{z}_7)$ goes behind two strands from $\tilde{z}_1$ to $\tilde{z}_2$ and from $\tilde{z}_2$ to $\tilde{z}_3$, and goes around the rear side of the cylinder. Using the generators of the braid, the type of the braid displayed in Fig. 5 is represented as

$$\beta_{2/7} = \sigma_1^{-1}\sigma_2^{-1}\sigma_4^{-1}\sigma_5^{-1}\rho_{2/7}, \tag{4·2}$$

$$\sim \sigma_1^{-1}\sigma_2^{-1}\sigma_2^{-1}\sigma_3^{-1}\rho_{2/7}. \tag{4·3}$$

Here, $\rho_{2/7} = (\sigma_6\sigma_5\sigma_4\sigma_3\sigma_2\sigma_1)^2$ is the braid type of 2/7-B. In order to derive the representation in Eq. (4·3), the Reidemeister moves and the Markov moves are repeatedly performed. Symbol '$\sim$' in Eq. (4·3) indicates the equivalence between two braid types.

We now show that orbital motions deviating from the rigid motion approximation do not affect the topological entropy of braids. Let us consider the braid type $\beta_{p/q}$ obtained by the rigid motion approximation. Suppose two adjacent orbital points $\tilde{z}_i$ and $\tilde{z}_j$ in the cylinder are in $0 \leq x < \pi$, and $\pi_x(\tilde{z}_i) < \pi_x(\tilde{z}_j)$. In addition, we suppose that $\tilde{z}_i$ and $\tilde{z}_j$ are included in the different resonance chains. If, in the rigid motion approximation, $\pi_x(\tilde{z}_j) < \pi_x(\tilde{z}_i)$, then we revolve $\tilde{z}_i$ and $\tilde{z}_j$ clockwise (as seen from above) by angle π around the vertical axis between them. As a result, generator σ_l^{-1} appears in front of $\beta_{p/q}$.

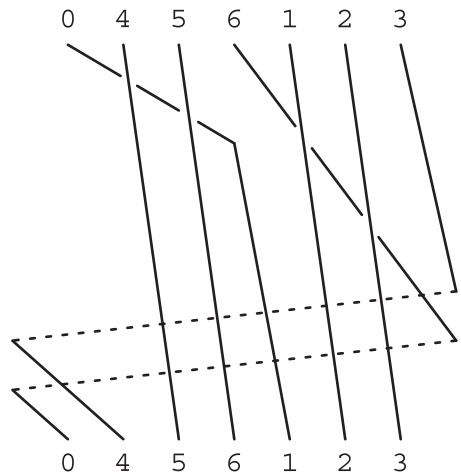

Fig. 5. Braid for $1/5 \oplus 1/2$-NB. Symbol i stands for $\tilde{z}_i$.

Because of reversibility, we must exchange the two positions $\tilde{z}_{q-j}$ and $\tilde{z}_{q-i}$. Then, generator σ_l appears after $\beta_{p/q}$. After this exchange, we have a new braid type, $\sigma_l^{-1}\sigma_{l'}^{-1}\beta_{p/q}\sigma_l\sigma_{l'}$. Since the relation $l'-l \geq 2$ holds, this braid type is equivalent to $\beta_{p/q}$. There are two restrictions imposed on the possible deviations from the rigid motion approximation owing to the reversibility of the map. First, the position of $\tilde{z}_0$ is uniquely determined. Therefore, we cannot exchange $\tilde{z}_0$ with other points. Second, we cannot exchange two adjacent orbital points $\tilde{z}_m$ and $\tilde{z}_n$ [$m = 6$ and $n = 1$ in Fig. 5] such that $0 \leq \pi_x(\tilde{z}_m) < \pi$ and $\pi \leq \pi_x(\tilde{z}_n) < 2\pi$. Then, we can obtain an actual permutation order from the simplest permutation order by repeated use of the above exchange without affecting the value of the topological entropy.

Now, let us take the sequence $1/(2k+1) \oplus 1/2$-NB ($k = 1, 2, \ldots$). The permutation order for each NB is $\mathrm{Perm}(1/(2k+1) \oplus 1/2) = (0, k+2, k+3, \cdots, 2k+2, 1, 2, \cdots, k+1)$. Then, we have the following braid type for each k,

$$\beta_{2/(2k+3)} = \epsilon_k \rho_{2/(2k+3)}, \tag{4·4}$$

$$\epsilon_k = \sigma_1^{-1}\sigma_2^{-1}\cdots\sigma_k^{-1}\sigma_k^{-1}\sigma_{k+1}^{-1}\cdots\sigma_{2k-1}^{-1}, \tag{4·5}$$

$$\rho_{2/(2k+3)} = (\sigma_{2k+2}\sigma_{2k+1}\cdots\sigma_1)^2. \tag{4·6}$$

Using the Burau matrix method and the program in Ref. 14), we can derive the characteristic equation for the eigenvalues,

$$(\lambda+2)(\lambda^{2k}+2) = 3. \tag{4·7}$$

In the limit $k \to \infty$, the largest value $\lambda_{\max}$ of absolute eigenvalues tends to $\lambda_{\max} = 2$. Thus, the topological entropy in the situation displayed in Fig. 1(a) is $\ln 2$. This is consistent with the result obtained in Ref. 5).

Next, we consider the situation displayed in Fig. 1(b). In this situation, $p_k/q_k \oplus r_k/s_k$-NB exists, where $0 < p_k/q_k < r_k/s_k < 1$ holds. We let $p_k = 1, q_k = 2k+1$, $r_k = 2k-1$ and $s_k = 2k$ for $k \geq 1$. Using the same procedure as mentioned above, we construct the braid and obtain its braid type $\beta_{2k/(4k+1)}$. For example, the braid of $\beta_{4/9}$ is displayed in Fig. 6, where $\beta_{4/9} = \sigma_5^{-1}\sigma_6^{-1}\sigma_3^{-1}\sigma_4^{-1}\sigma_5^{-1}\sigma_1^{-1}\sigma_2^{-1}\sigma_3^{-1}\rho_{4/9}\sigma_3^{-1}\sigma_4^{-1}\sigma_5^{-1}\sigma_2^{-1}$ and $\rho_{4/9} = (\sigma_8\cdots\sigma_1)^4$. The following characteristic equation is obtained:

$$(1+\lambda-\lambda^2) + \lambda^6(\lambda^2+\lambda-1) + 3\lambda^3(\lambda^2-\lambda+1) = 0. \tag{4·8}$$

Thus, we have $\lambda_{\max} = 2.3340\cdots$.

The general representation of braid types for large k is very complicated and thus is omitted. We give the following characteristic equation for $\beta_{2k/(4k+1)}$ ($k \geq 3$).

$$\begin{aligned}(1+\lambda-\lambda^2) + \lambda^{4k-2}(\lambda^2+\lambda-1) \\ + (\lambda-1)\sum_{m=1}^{k-2}(2m+1)(\lambda^{4k-2m-2} - \lambda^{2m+1}) \\ + (2k-1)\lambda^{2k-1}(\lambda^2-\lambda+1) = 0.\end{aligned} \tag{4·9}$$

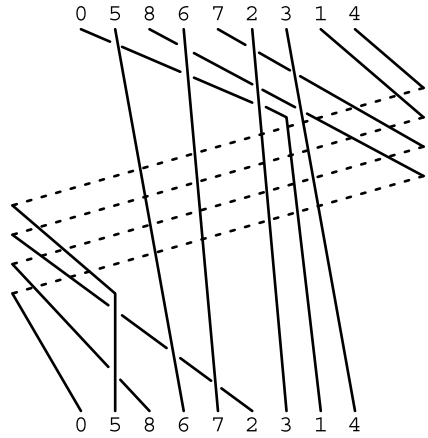

Fig. 6. Braid for $1/5 \oplus 3/4$-NB for $k = 2$.

In the limit $k \to \infty$, the highest divergent terms are proportional to λ^{4k}. Gathering these terms, we have the following coefficient of λ^{4k},

$$\frac{\lambda(\lambda^2 + 2\lambda - 1)}{(\lambda^2 - 1)(\lambda + 1)}. \tag{4·10}$$

In the limit $k \to \infty$, the largest value of absolute eigenvalues tends to $\sqrt{2} + 1$.

§5. Topological entropies for various trellises

Using the method in §4, we calculate $\lambda_{\max}$ for trellises. We give our results in Table I. In the table, the first column shows the type of trellis $\mathcal{T}$, the second column lists the NBs forced by $\mathcal{T}$, the third column shows the corresponding $\lambda_{\max}$, and the fourth column shows the critical parameter value a_c, at which the trellis appears.

Several technical notes are in order for the calculation of $\lambda_{\max}$ and a_c. We use $p/q \oplus r/s$-NBs for a given irreducible r/s. The smaller the value of p/q the better, that is, $p/q \oplus r/s$-NBs bifurcate at larger parameter values if p/q is smaller. Hence, we let p be 1. Using the permutation order of the orbital points of $1/q \oplus r/s$-NB, we construct the braid. As for $1/q$, we set $\mathrm{GCM}(q, s) = 1$, where q is odd (even) if s is even (odd). According to the rigid motion approximation with $\mathrm{GCM}(q, s) = 1$, there are no pairs of points whose $\tilde{x}$-coordinates are the same. We have calculated the value of the eigenvalue up to four significant figures. In order for this, it has been sufficient that the period $q + s$ is approximately equal to 30. For example, the eigenvalue for the braid type of $1/18 \oplus 2/5$-NB is 1.80367 and that of $1/24 \oplus 2/5$-NB is 1.80370. Thus, we have the eigenvalue 1.803 for the situation satisfying $T^2\Gamma \cap S_H(3) \neq \emptyset$. Next, we draw the graphs of Γ_u and the backward image of the symmetry axis. We determine the value of a_c at which the two graphs have the first tangency point.

The topological entropy tends to zero in the limit $a \to 0$. In fact, let $h_{\mathrm{top}}(p/q)$ be the topological entropy of p/q-NB. We use the fact that $h_{\mathrm{top}}(p/q)$ is $O(1/q)$ for the limit $p/q \to 0$.[17] On the other hand, the critical value $a_c(p/q)$ decreases to zero in the limit $p/q \to 0$.

Table I.

Trellis $\mathcal{T}$	Non-Birkhoff periodic orbit	$\lambda_{\max}$	a_c
Trellis of Fig. 1(b)	$p/q \oplus r/s$-NB $(0 < p/q < r/s < 1)$	$\sqrt{2}+1$	3.368
$T^2\Gamma_u \cap S_G(6) \neq \emptyset$	$p/q \oplus 5/6$-NB $(0 < p/q < 5/6)$	2.405	3.367
$T^2\Gamma_u \cap S_H(5) \neq \emptyset$	$p/q \oplus 4/5$-NB $(0 < p/q < 4/5)$	2.392	3.365
$T^4\Gamma_u \cap S_H(8) \neq \emptyset$	$p/q \oplus 7/9$-NB $(0 < p/q < 7/9)$	2.382	3.361
$T\Gamma_u \cap S_G(4) \neq \emptyset$	$p/q \oplus 3/4$-NB $(0 < p/q < 3/4)$	2.359	3.352
$T^5\Gamma_u \cap S_H(9) \neq \emptyset$	$p/q \oplus 8/11$-NB $(0 < p/q < 8/11)$	2.335	3.327
$T^3\Gamma_u \cap S_H(6) \neq \emptyset$	$p/q \oplus 5/7$-NB $(0 < p/q < 5/7)$	2.333	3.326
$T^4\Gamma_u \cap S_G(8) \neq \emptyset$	$p/q \oplus 7/10$-NB $(0 < p/q < 7/10)$	2.331	3.324
$T\Gamma_u \cap S_H(3) \neq \emptyset$	$p/q \oplus 2/3$-NB $(0 < p/q < 2/3)$	2.269	3.289
$T^5\Gamma_u \cap S_H(8) \neq \emptyset$	$p/q \oplus 7/11$-NB $(0 < p/q < 7/11)$	2.205	3.147
$T^3\Gamma_u \cap S_G(6) \neq \emptyset$	$p/q \oplus 5/8$-NB $(0 < p/q < 5/8)$	2.204	3.146
$T^6\Gamma_u \cap S_H(9) \neq \emptyset$	$p/q \oplus 8/13$-NB $(0 < p/q < 8/13)$	2.203	3.144
$T^2\Gamma_u \cap S_H(4) \neq \emptyset$	$p/q \oplus 3/5$-NB $(0 < p/q < 3/5)$	2.190	3.141
$T^5\Gamma_u \cap S_G(8) \neq \emptyset$	$p/q \oplus 7/12$-NB $(0 < p/q < 7/12)$	2.177	3.136
$T^3\Gamma_u \cap S_H(5) \neq \emptyset$	$p/q \oplus 4/7$-NB $(0 < p/q < 4/7)$	2.174	3.129
$T^4\Gamma_u \cap S_H(6) \neq \emptyset$	$p/q \oplus 5/9$-NB $(0 < p/q < 5/9)$	2.171	3.127
$\Gamma_u \cap S_G(2) \neq \emptyset$	$p/q \oplus 1/2$-NB $(0 < p/q < 1/2)$	2	2.920
$T^4\Gamma_u \cap S_H(5) \neq \emptyset$	$p/q \oplus 4/9$-NB $(0 < p/q < 4/9)$	1.836	2.157
$T^3\Gamma_u \cap S_H(4) \neq \emptyset$	$p/q \oplus 3/7$-NB $(0 < p/q < 3/7)$	1.829	2.155
$T^5\Gamma_u \cap S_G(6) \neq \emptyset$	$p/q \oplus 5/12$-NB $(0 < p/q < 5/12)$	1.823	2.146
$T^2\Gamma_u \cap S_H(3) \neq \emptyset$	$p/q \oplus 2/5$-NB $(0 < p/q < 2/5)$	1.803	2.134
$T^6\Gamma_u \cap S_H(6) \neq \emptyset$	$p/q \oplus 5/13$-NB $(0 < p/q < 5/13)$	1.783	2.091
$T^3\Gamma_u \cap S_G(4) \neq \emptyset$	$p/q \oplus 3/8$-NB $(0 < p/q < 3/8)$	1.779	2.087
$T^5\Gamma_u \cap S_H(5) \neq \emptyset$	$p/q \oplus 4/11$-NB $(0 < p/q < 4/11)$	1.775	2.079
$T\Gamma_u \cap S_H(2) \neq \emptyset$	$p/q \oplus 1/3$-NB $(0 < p/q < 1/3)$	1.695	1.984
$T^4\Gamma_u \cap S_G(4) \neq \emptyset$	$p/q \oplus 3/10$-NB $(0 < p/q < 3/10)$	1.614	1.632
$T^3\Gamma_u \cap S_H(3) \neq \emptyset$	$p/q \oplus 2/7$-NB $(0 < p/q < 2/7)$	1.603	1.625
$T^5\Gamma_u \cap S_H(4) \neq \emptyset$	$p/q \oplus 3/11$-NB $(0 < p/q < 3/11)$	1.591	1.594
$T\Gamma_u \cap S_G(2) \neq \emptyset$	$p/q \oplus 1/4$-NB $(0 < p/q < 1/4)$	1.543	1.533
$T^4\Gamma_u \cap S_H(3) \neq \emptyset$	$p/q \oplus 2/9$-NB $(0 < p/q < 2/9)$	1.489	1.316
$T^2\Gamma_u \cap S_H(2) \neq \emptyset$	$p/q \oplus 1/5$-NB $(0 < p/q < 1/5)$	1.451	1.257
$T^2\Gamma_u \cap S_G(2) \neq \emptyset$	$p/q \oplus 1/6$-NB $(0 < p/q < 1/6)$	1.387	1.063

§6. Order relations for the connecting orbits

We have shown[18] the existence of Mather's connecting orbits in the standard map. In this section, we consider sequences of connecting orbits, and obtain homoclinic or heteroclinic orbits as their limits. A topological entropy is associated with each connecting orbit. If we consider a sequence of connecting orbits which is monotone in the topological entropy, then we can assign a unique entropy value to a homoclinic or heteroclinic orbit obtained as a limit. Then this entropy value may be taken as the entropy of the system in which the corresponding homoclinic or heteroclinic orbit exists.

Consider the two sequences $\{p_k/q_k\}$ and $\{r_k/s_k\}$ of irreducible fractions satisfying the conditions $0 < p_k/q_k < r_k/s_k < 1$, $p_{k+1}/q_{k+1} < p_k/q_k$, $r_k/s_k < r_{k+1}/s_{k+1}$, $\lim_{k\to\infty} p_k/q_k = 0/1$ and $\lim_{k\to\infty} r_k/s_k = 1/1$. First, we consider the orbital struc-

ture of $p_k/q_k \oplus 1/2$-NB in the limit $k \to \infty$. The forward orbit accumulates at saddle $P_{1,0}$, and the backward orbit at saddle $P_{0,0}$. In addition, the orbit has a point in the resonance region of $\langle Z_{1/2} \rangle$. This is a homoclinic orbit of $P_{0,0}$ since $P_{0,0} = P_{1,0}$ in the cylinder. We call this the homoclinic connecting orbit $\mathcal{H}_{P_{0,0}}(1/2)$. Similarly, the homoclinic connecting orbit named $\mathcal{H}_{P_{0,0}}(p/q)$ for any irreducible p/q with $0 < p/q < 1$ is defined.

Next, we consider the orbital structure of $p_k/q_k \oplus r_k/s_k$-NB in the limit $k \to \infty$. The forward orbit accumulates at saddle $P_{0,1}$ and the backward orbit at saddle $P_{0,0}$ in the cylinder. Thus, this is a heteroclinic orbit connecting $P_{0,0}$ and $P_{0,1}$. We denote this orbit by $\mathcal{H}(0/1, 1/1)$. As mentioned in §§4 and 5, the existence of a connecting orbit implies chaos. Therefore, we can assign a positive topological entropy to the connecting orbit. We give the following order relations among the homoclinic and heteroclinic connecting orbits,

$$\mathcal{H}(0/1, 1/1) \to \mathcal{H}_{P_{0,0}}(r/s) \to \mathcal{H}_{P_{0,0}}(p/q) \text{ for } 0 < p/q < r/s < 1/1. \tag{6·1}$$

Here, we read $\mathcal{H}_{P_{0,0}}(r/s) \to \mathcal{H}_{P_{0,0}}(p/q)$ as $\mathcal{H}_{P_{0,0}}(r/s)$ forces $\mathcal{H}_{P_{0,0}}(p/q)$. The order relation means that $\mathcal{H}_{P_{0,0}}(p/q)$ exists if $\mathcal{H}_{P_{0,0}}(r/s)$ exists in the system. From the order relations, the homoclinic connecting orbit for every p/q $(0 < p/q < 1)$ exists if $\mathcal{H}(0/1, 1/1)$ exists in the system.

Acknowledgements

The authors are grateful for the useful comments of the referees.

References

1) P. Collins, Int. J. Bifurcation and Chaos **12** (2002), 605.
2) T. Matsuoka, Contemp. Math. **152** (1993), 229.
3) Y. Yamaguchi and K. Tanikawa, Prog. Theor. Phys. **114** (2005), 763.
4) Y. Yamaguchi and K. Tanikawa, Prog. Theor. Phys. **114** (2005), 1163.
5) Y. Yamaguchi and K. Tanikawa, Prog. Theor. Phys. **107** (2002), 1117.
6) M. Bestvina and M. Handel, Topology **34** (1995), 109.
7) T. Hall, *Trains3* was obtained from the following website: `http://www.liv.ac.uk/maths/PURE/MIN_SET/CONTENT/members/T_Hall.html`
8) Y. Yamaguchi and K. Tanikawa, Prog. Theor. Phys. **117** (2007), 601.
9) R. de Vogelaere, in *Contribution to the Theory of Nonlinear Oscillation*, Vol. IV, ed. S. Lefschetz (Princeton University Press, 1958), p. 53.
10) K. R. Mayer and G. R. Hall, *Introduction to Hamiltonian Dynamical Systems and the N-Body Problem* (Springer-Verlag, 1991), Chap. X.
11) G. D. Birkhoff, Trans. Amer. Math. Soc. **14** (1913), 14; Acta. Math. **47** (1925), 297.
12) R. S. Mackay and J. D. Meiss, Phys. Lett. A **98** (1983), 92.
13) S. Aubry, Physica D **7** (1983), 240.
14) S. Aubry and P. Y. Le Daeron, Physica D **8** (1983), 381.
15) P. Boyland, Contemp. Math. **81** (1988), 119.
16) P. Boyland, Topology and Its Applications **58** (1994), 223
17) E. Hironaka and E. Kin, Algebraic and Geometric Topology **6** (2006), 699.
18) Y. Yamaguchi and K. Tanikawa, Prog. Theor. Phys. **119** (2008), 533.